ADDRESSING CONFOUNDS IN FUNCTIONAL CONNECTIVITY ANALYSES OF CALCIUM IMAGING

Dingding Ye*1, Charan Santhirasegaran*2, Ryan Pai*1, Genevera I. Allen1, Joseph Young1

¹Rice University ²Columbia University jy46@rice.edu

ABSTRACT

Elucidating functional connectivity reveals interactions between brain regions based on their in vivo activity. However, a gap exists in current statistical methods' ability to untangle direct interactions from confounding activity due to stimuli and physiological effects, leading to a bottleneck in understanding how the brain filters and decodes information. We propose methods to remove physiological and environmental effects from calcium imaging in the rodent olfactory bulb to better isolate connectivity-related activity correlations. Our approach deconvolves brain signals by learning smooth filters leveraging generalized ridge regularization, thus producing stronger isolation of such connectivity-related activity. Our method for removing specific external correlation-causing factors is applicable in a wide variety of settings including those with different external stimuli.

Index Terms— functional connectivity, ridge regression, calcium imaging, olfaction

1. INTRODUCTION

Functional connectivity, the correlation in neural activity between spatially distinct areas, is an important tool for understanding brain structure and function [1]. Mapping functional connectivity allows analysis of how parts of the brain play related and interdependent roles in various cognitive and physiological processes [1] [2]. Functional connectivity differs from effective connectivity analyses, which take into account a priori assumptions about neurophysiology and the models used to describe it. Because functional connectivity is only concerned with correlation in activity and not with any prior knowledge, it is readily applicable and also brings an added benefit of being able to find relationships between regions with undiscovered connections. A commonly mentioned drawback of functional connectivity analyses is that relationships may be found that are correlative but not causative. However, functional connectivity analyses may reveal certain neural phenomena that are not necessarily causative, such as parallel processing in the brain.

The olfactory system is a particularly interesting sensory system of the brain within which to perform functional connectivity analyses for several reasons. Firstly, it is the only sensory system that relays data directly to the primary site of sensory processing instead of being routed through the thalamus [3]. Secondly, it is the least understood and phylogenetically oldest sensory pathway and it remains unknown how features are spatially arranged in the olfactory bulb (OB) and whether they are processed in parallel as they are in other sensory systems [3]. Thirdly, the relatively strong influence

THIS WORK WAS SUPPORTED BY A TRAINING FELLOWSHIP FROM THE GULF COAST CONSORTIA, ON THE IGERT: NEUROENGINEERING FROM CELLS TO SYSTEMS, NATIONAL SCIENCE FOUNDATION (NSF) 1250104, AND BY NATIONAL INSTITUTES OF HEALTH (NIH) GRANTS U01NS108680 AND R01DC013802.

of the olfactory bulb on emotion and memory caused by its direct connections to the amygdala, hippocampus, and medial prefrontal cortex make it a compelling system to study [4]. A basic diagram of the olfactory system is shown below in Figure 1(a).

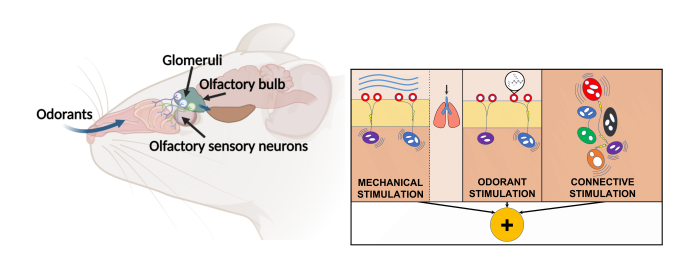


Fig. 1: (a) Diagram of the rodent olfactory system (left). (b) Illustration of the factors that contribute to the recorded neural activity (right). Activity caused by mechanical and odorant stimulation is isolated and removed by our technique, better isolating activity caused by connectivity. (a) was created with Biorender.

While the OB is a fascinating topic of study, difficulties arise in resolving connectivity because OB recordings are contaminated by external influences. Breathing [5] and exposure to stimuli introduce correlations in the data that are unrelated to connectivity, thus posing the problem of how to separate connectivity-based correlations from other physiological causes of correlation. The problem of physiological noise in neural recordings has been significantly addressed in functional magnetic resonance imaging (fMRI) [6,7], and we use that work as inspiration to address the aforementioned confounds in OB recordings.

The data we analyzed is from OB calcium imaging, which is a popular method of acquiring neural activity due to the fact that changes in calcium concentrations are a strong indication of neural activity. These recordings are taken from glomeruli, which are spherical bundles of synapses between olfactory nerves and projection neurons including tufted and mitral cells [8]. Because of the popularity of calcium imaging, extending the work done on isolating factors of correlation in fMRI to calcium imaging has potential to reveal structural correlations even beyond the OB.

2. EXPERIMENTAL PROCEDURE

All animal procedures were conducted in accordance with an animal protocol that was approved by the Institutional Animal Care and Use Committee (IACUC) of The University of Texas Health Science Center at Houston (UTHealth). The following steps are also mentioned in a prior work [9], however the spontaneous (no odorant) data collected was used in the prior work [9] while we use the stimulus (odorant) data for the present work. Further note that the lab technique in [10] is nearly identical to the technique of this work and the prior work [9].

indicates equal contribution.

For conducting calcium imaging, researchers anesthetized a mouse (male; 5 months old at imaging) with lineage of Gad2-IRESCre [11] (JAX stock #10802) and RCL-tdTomato [12] (Ai9; JAX stock #7909). In order to achieve genetically-encoded calcium indicator GCaMP6f expression by the synapsin promoter in OB neurons, AAV vector (AAV1.Syn.GCaMP6f.WPRE.SV40; UPenn Vector Core) was given to the mouse three weeks before imaging.

During the procedure, an anesthetic (urethane; 6% w/v, 20 µl/g bodyweight) was administered to the mouse and reinforced upon toe pinch reaction by the mouse. Additionally, a heating pad held the mouse body temperature constant at a 36-37 °C range. Then, imaging was conducted through the exposure of the skull over the dorsal OB to create a cranial window. The equipment used included an acousto-optic deflector-based two-photon microscope equipped with a Nikon 16x/0.8NA objective lens with random-access mode imaging available.

For a more focused analysis, regions of interest (ROIs) in the mouse OB were selected through a process of determining the loci of glomeruli by triggering responses to certain odors. After the identification of these locations, the ROIs were put at each glomerulus' middle region to minimize the possibility of interference of surrounding cell bodies. From the ten glomeruli detected, two ROIs were selected per glomerulus and imaged with a 500 Hz sampling rate. Simultaneous to imaging, a chest-placed piezo-electric captured breathing. Overall, the data gathered includes ROI and breathing data for multiple 15-second segments where an odorant stimulus was introduced. The pairs of ROIs for each glomerulus were averaged to yield the glomerular time series data.

3. MODELING OLFACTORY BULB CONNECTIVITY

3.1. Modeling Olfactory Bulb Signals

We represent glomerular activity as the linear combination of three independent components: breathing, odorant response, and noisy glomerular connectivity, as illustrated in Figure 1(b). Inspired by the fMRI literature [6, 7], we learn linear and time-invariant filters to model the effects of both breathing and stimuli, allowing us to isolate each of the three components of the data. Filtering out breathing-related activity allows for analysis of spatial organization of responses to different odorant stimuli. Further filtering out stimulus responses results in isolated noisy connectivity-related activity, which can finally be analyzed to infer functional connectivity more accurately than with the original data.

Mathematically, the recorded time-series for a single glomerulus j is represented as an N-length vector,

$$\mathbf{y}_j = \left[y_j[1] \cdots y_j[n] \cdots y_j[N]\right]^\top,$$

where time is indexed by n. The signals for different glomeruli u and v should not be directly analyzed via correlation (e.g., as $\mathbf{y}_u \cdot \mathbf{y}_v$) prior to the removal of confounds because this will tend to reveal correlation between glomeruli which have similar responses to mechanical stimulation from breathing [5] and to chemical stimulation from odorants. Thus, in order to determine more precise functional connectivity between glomeruli, the components of each glomerulus time series which derive from mechanical and odorant stimulation must be removed.

The purpose of our model, which is inspired by prior work in fMRI [6], is to perform a decomposition for every \mathbf{y}_j into three components: \mathbf{g}_j , the component due to mechanical stimulation from breathing, \mathbf{h}_j , the component due to odorant stimulation, and \mathbf{r}_j , the residual noisy connectivity component. Hence, the decomposition is represented as $\mathbf{y}_j = \mathbf{g}_j + \mathbf{h}_j + \mathbf{r}_j$. The components \mathbf{h}_j and \mathbf{g}_j were each modeled as the output of causal linear and time-invariant filters applied to the breathing and odorant time-series data, respec-

tively. The breathing filter weights are represented as a vector $\boldsymbol{\phi}_{j}^{(b)}$, of length γ , and the odorant filter weights as $\boldsymbol{\phi}_{j}^{(o)}$, of length η .

The final component \mathbf{r}_j was assumed to be zero-mean Gaussian. At any time index n, all glomeruli can be represented by the random vector $\mathbf{r}[n]$ containing the residuals of all glomeruli, and $\mathbf{r}[n]$ has a multivariate Gaussian distribution. This distribution encapsulates the covariance of residuals between the K glomeruli, where specifically $\mathbf{r}[n] = [r_1[n] \cdots r_j[n] \cdots r_K[n]] \sim \mathcal{N}(\mathbf{0}, \mathbf{\Sigma})$. The diagonal of the covariance matrix $\mathbf{\Sigma}$ describes the noise of glomerular residuals while the off-diagonal elements contain the desired breathing- and stimulus-adjusted covariances related to glomerular functional connectivity.

3.2. Breathing and Stimulus Filtering

We seek to estimate smooth, linear and time-invariant filters, $\phi_i^{(b)}$ and $\pmb{\phi}_i^{(o)}$ representing the weights of the breathing and odorant filters respectively. To achieve this, first let $\mathbf{X} = [\mathbf{X}^{(b)} \ \mathbf{X}^{(o)}]$, where $\mathbf{X}^{(b)}$ and $\mathbf{X}^{(o)}$ are the Toeplitz matrices for the convolution performed by the linear and time invariant filters consisting of row-wise staggered and windowed versions of the breathing and stimulus data, respectively. We propose to learn the smooth filter weights via generalized ridge regression [13, 14] that uses a penalty to ensure not only low prediction error but also weight smoothness [6, 15] for both the breathing and stimulus filters. As in the fMRI literature, filter smoothness was assumed to ensure that the filters may be physiologically possible [6], because a filter whose output varies extremely strongly with even minuscule variations in relative input timing is unlikely to occur naturally. This results from the correlation that one expects to exist from one time point to another in biological time series. The linear and time-invariant confound filter weights are contained in the length $\nu = \gamma + \eta$ vector $\boldsymbol{\phi}_j = \left[\boldsymbol{\phi}_j^{(b)^\top} \ \boldsymbol{\phi}_j^{(o)^\top} \right]^\top$. Further, we define the smoothing matrix as the squared differences matrix $\mathbf{D}_{i}^{(\lambda)}$ as

$$\mathbf{D}_{j}^{(\lambda)} = \begin{bmatrix} \lambda_{j}^{(b)} \mathbf{M}_{b}^{\top} \mathbf{M}_{b} & \mathbf{0}_{\gamma \times \eta} \\ \mathbf{0}_{\eta \times \gamma} & \lambda_{j}^{(o)} \mathbf{M}_{o}^{\top} \mathbf{M}_{o} \end{bmatrix},$$

where $\lambda_j^{(b)}$ and $\lambda_j^{(o)}$ are the experimentally-determined ridge parameters, and \mathbf{M}_b and \mathbf{M}_o are the second-differences matrices to be applied to $\boldsymbol{\phi}_j^{(b)}$ and $\boldsymbol{\phi}_j^{(o)}$, respectively. Inspired by previous work on learning smooth filters [6, 13, 15], we propose to learn our smooth confounding filters via the following optimization:

$$oldsymbol{\phi}_j = \min_{oldsymbol{\phi}_j \in \mathbb{R}^
u} rac{1}{N} \|\mathbf{y}_j - \mathbf{X} oldsymbol{\phi}_j\|_2^2 + oldsymbol{\phi}_j^ op \mathbf{D}_j^{(\lambda)} oldsymbol{\phi}_j.$$

The typical ridge penalty penalizes the magnitude of filter weights, but the version of ridge regression we used penalizes the result of both second-differences matrices applied to the filter weights, ensuring filter smoothness in both the breathing and stimulus filters. The well-known analytical solution to the ridge regression problem was used to solve for the filter weights [6, 15]:

$$\phi_j = \left(\mathbf{X}^{\top} \mathbf{X} + N \mathbf{D}_j^{(\lambda)}\right)^{-1} \mathbf{X}^{\top} \mathbf{Y}.$$

In order to perform ridge regression, the ridge parameters $\lambda_j^{(b)}$ and $\lambda_j^{(o)}$ must be experimentally determined. Generalized cross-validation (GCV) was used to yield both parameters because ordinary cross-validation would prove too computationally expensive [16]. Both parameters were selected from a range of 7 exponentially spaced powers of 10, ranging from 10^0 to 10^6 inclusive, to balance

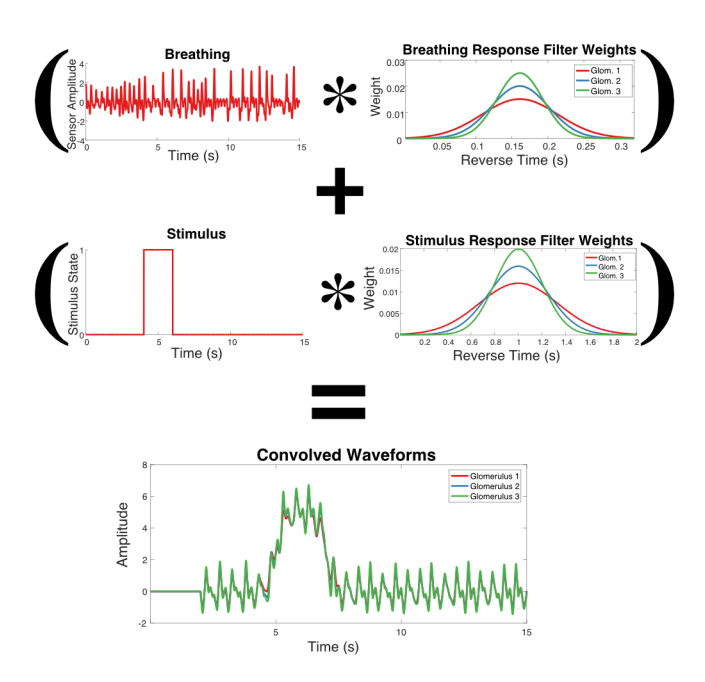


Fig. 2: Generation of simulated data through convolution of breathing and stimulus time series with simulated linear and time-invariant filters.

computational complexity with a wide range of parameter magnitudes. The GCV process is performed collectively for both ridge parameters in minimizing the mean squared error since we are simultaneously using breathing and odorant time series data. In other words, the overall process selects optimal parameters $\lambda_j^{(b)}$ and $\lambda_j^{(o)}$ and filter weights $\phi_j^{(b)}$ and $\phi_j^{(o)}$ for both breathing and odorant responses simultaneously.

3.3. Inferring Connectivity

Finally, we inferred functional connectivity using two commonly employed approaches to assess functional brain connectivity [17]: correlation and partial correlation. Specifically, we used the Pearson correlation coefficient to calculate the degree of correlation between the residual signals of pairs of glomeruli, \mathbf{r}_u and \mathbf{r}_v , for each possible pairing $\{u,v\}$. We additionally used the partial correlation [18] to capture the conditional correlation between pairs of glomeruli.

4. RESULTS

In vivo respiratory data from mice were recorded to validate the methods outlined in Section III. Substantial extraneous influences (i.e. breathing and odorant stimulus responses) were successfully removed with the proposed method to reveal underlying glomerular functional connectivity.

The model was first validated using simulated data only. As shown in Figure 2, the breathing and stimulus data were convolved with the corresponding simulated breathing $\phi_j^{(b)}$ and stimulus $\phi_j^{(c)}$ filters and ultimately combined to create the simulated time series. The model was then applied to this data to derive breathing and stimulus filters, which were found to accurately represent the filter weights.

As part of the validation process for the filter determination method, the effectiveness of the learned filter weights was compared

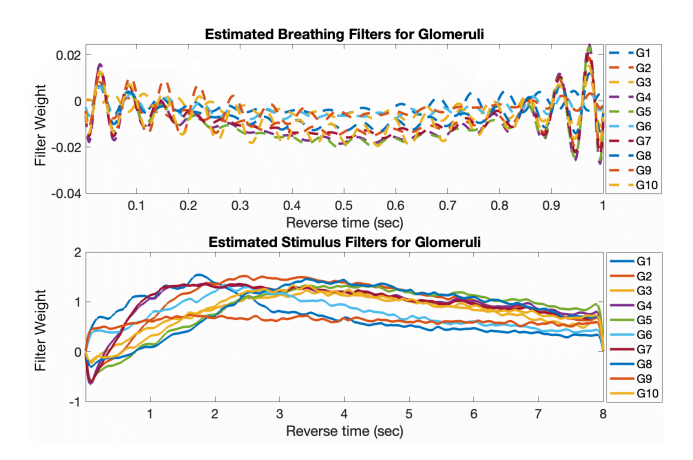


Fig. 3: Derived glomerulus-specific breathing and stimulus filters for real data for the 10 observed glomeruli. Filters have been displayed on the same plot to allow comparison of glomerular responses to breathing and introduction of stimulus.

to different filter weights produced by arbitrary λ values rather than λ values selected by GCV. It was demonstrated that the learned weights accurately represented the true data values, whereas the arbitrary weights failed to do so.

Following the successful validation using simulated data, the method was applied to the real stimulus data. The analysis, as expected, revealed the identification of stimulus filters that demonstrated a decrease in influence over time as illustrated in Figure 3. The stimulus filters were designed to begin at the first intake of breath following the introduction of the stimulus, leading to a more pronounced impact on the data than that of the breathing filters. The breathing filters in this instance appear less informative, which is expected because stimulus activity appears to dominate recordings when odorants are introduced. Furthermore, because both breathing and stimulus filters are constrained to be time-invariant, changes in the breathing response over time may be passed to the stimulus filter. As seen from Figure 4, the residual waveforms, which have been adjusted from the original recordings for both breathing and stimulus effects, can now be examined.

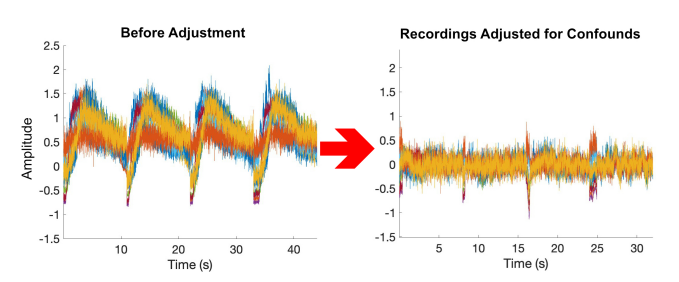


Fig. 4: Time series before and after removal of activity due to external causes. The absence of periodic and drastic increases in activity due to stimulus presentation is clear, while removal of breathing related response is not as obvious.

The waveform data was analyzed to infer glomerular connectivity using the Pearson correlation coefficient. The initial correlation plot in Figure 5 showed nearly uniformly strong pairwise correlations between glomeruli which lacked informative features due to commonality among glomeruli in terms of breathing and stimulus responses. Furthermore, inhibitive correlations between glomeruli were extremely uncommon. However, after adjusting for both breathing and stimulus response, the final plot (Fig. 5) revealed a

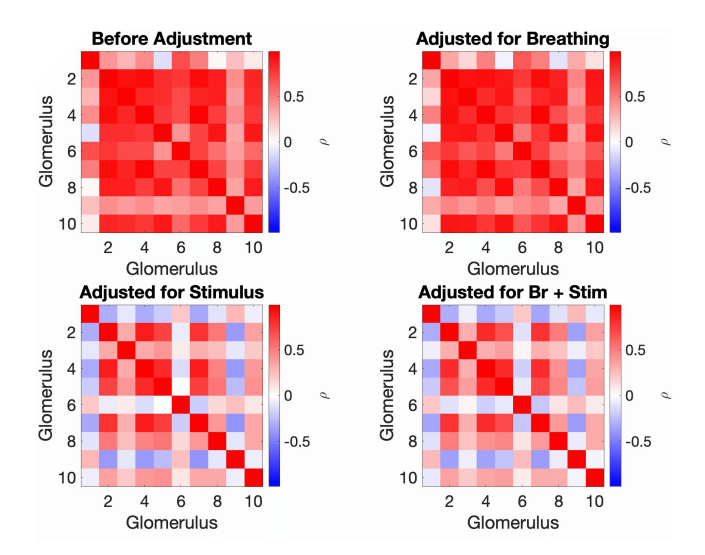


Fig. 5: Correlations between glomeruli at various stages of removal of stimulus and breathing related activity using the Pearson correlation coefficient. Some correlations become negative after removal of stimulus related activity possibly due to lateral inhibition between glomeruli.

notable increase in variation in correlation. This adjustment also unveiled negative correlations that were not initially apparent, indicating the potential influence of lateral inhibition [19] between glomeruli that was hidden by the noise of general stimulus-related activity.

The same process was performed using partial correlation (Fig. 6). As with the Pearson correlation, we often see decreases in correlation magnitude using partial correlation. However, also observable are changes in correlation sign again indicating that our decomposition is able to reveal connections that even partial correlation, when adjusting for the influence of common components found in other glomeruli, is not able to reveal. This contrast serves to demonstrate the effectiveness of the method in extracting meaningful relationships and underlying patterns from complex data, making it a powerful tool for further analysis and exploration.

Finally, we performed a brief analysis on the potential existence of a spatial relationship for connectivity between glomeruli (Fig. 7). We find that our breathing and stimulus adjusted partial correlation reveals stronger functional connections between a subset of spatially closer glomeruli. This is consistent with the previous findings of neurons in the visual cortex [20] and reveals important findings about the neural circuitry in the olfactory bulb. These preliminary findings can be more robustly tested over a larger set of glomeruli distributed over a greater area of the olfactory bulb to confirm our findings and reveal further relationships.

5. FINAL REMARKS

This method could be applied to a broad variety of problems that require isolation of the effects of external factors in order to study latent relationships hidden in the data. Further research could focus on comparing the efficacy of the proposed method to an unsupervised method such as functional principal components analysis (FPCA), which may provide a greater understanding of the benefits and drawbacks of relying on external data (such as stimulus or breathing data) to decouple the corresponding signals. The use of time-varying filters may also prove more effective in modeling the relationship between confounds and observed activity.

In addition to the work done in this manuscript centered on learn-

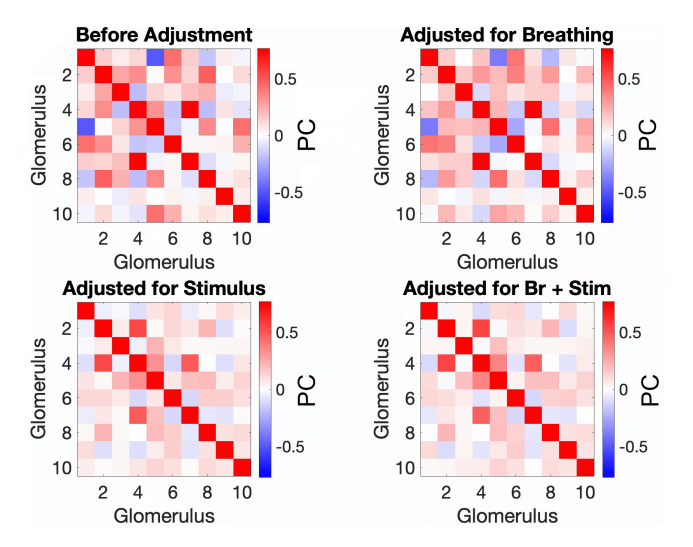


Fig. 6: Partial correlations between glomeruli at various stages of removal of stimulus and breathing related activity.

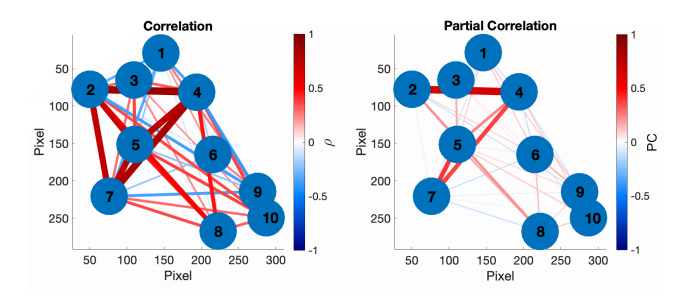


Fig. 7: Relationships between interglomerular distance and connection strength after removal of stimulus and breathing-related activity. Nodes indicate the approximate center of glomeruli in the calcium images taken of the olfactory bulb. Edges vary in color according to correlation coefficient, and edge widths vary according to correlation coefficient magnitude.

ing filters, future work could focus on better understanding how the brain distinguishes between odors, especially those that are similar. This could help determine whether the lateral inhibition suggested by the negative correlations is indeed responsible for enabling finer differentiation between similar scents [19]. One possible avenue for this research could be investigating how removing the largest principal components of the data affects the calculated connectivity. Additionally, applying this model to data including a large set of stimuli could help reveal correlations between glomeruli that would be missed when using a single odorant.

6. ACKNOWLEDGMENT

We thank Shin Nagayama and Ryota Homma for providing rodent data and feedback as well as Behnaam Aazhang for feedback. We used ColorBrewer [21] for color selection in a portion of the figures.

7. REFERENCES

- [1] Baxter P. Rogers, Victoria L. Morgan, Allen T. Newton, and John C. Gore, "Assessing functional connectivity in the human brain by fMRI," *Magnetic Resonance Imaging*, vol. 25, no. 10, pp. 1347–1357, Dec. 2007.
- [2] Yasaman Shahhosseini and Michelle F. Miranda, "Functional connectivity methods and their applications in fMRI data," *Entropy*, vol. 24, no. 3, pp. 390, Mar. 2022.
- [3] Dale Purves, George J. Augustine, David Fitzpatrick, Lawrence C. Katz, Anthony-Samuel LaMantia, James O. Mc-Namara, and S. Mark Williams, "The organization of the olfactory system," in *Neuroscience*. 2nd edition. Sinauer Associates, 2001.
- [4] Michael C. Farruggia, Robert Pellegrino, and Dustin Scheinost, "Functional connectivity of the chemosenses: A review," Frontiers in Systems Neuroscience, vol. 16, pp. 865929, June 2022.
- [5] Ryo Iwata, Hiroshi Kiyonari, and Takeshi Imai, "Mechanosensory-based phase coding of odor identity in the olfactory bulb," *Neuron*, vol. 96, no. 5, pp. 1139 – 1152.e7, 2017
- [6] Catie Chang, John P. Cunningham, and Gary H. Glover, "Influence of heart rate on the BOLD signal: The cardiac response function," *NeuroImage*, vol. 44, no. 3, pp. 857–869, 2009.
- [7] Rasmus M. Birn, Monica A. Smith, Tyler B. Jones, and Peter A. Bandettini, "The respiration response function: The temporal dynamics of fMRI signal fluctuations related to changes in respiration," *NeuroImage*, vol. 40, no. 2, pp. 644–654, 2008.
- [8] Alison Maresh, Diego Rodriguez Gil, Mary C. Whitman, and Charles A. Greer, "Principles of glomerular organization in the human olfactory bulb – Implications for odor processing," *PLOS ONE*, vol. 3, no. 7, pp. e2640, July 2008, Publisher: Public Library of Science.
- [9] Joseph Young, Ryota Homma, and Behnaam Aazhang, "Addressing indirect frequency coupling via partial generalized coherence," *Scientific Reports*, vol. 11, no. 1, pp. 6535, Mar 2021.
- [10] Ryota Homma, Xiaohua Lv, Tokiharu Sato, Fumiaki Imamura, Shaoqun Zeng, and Shin Nagayama, "Narrowly confined and glomerulus-specific onset latencies of odor-evoked calcium transients in the juxtaglomerular cells of the mouse main olfactory bulb," eNeuro, vol. 6, no. 1, 2019.
- [11] Hiroki Taniguchi, Miao He, Priscilla Wu, Sangyong Kim, Raehum Paik, Ken Sugino, Duda Kvitsani, Yu Fu, Jiangteng Lu, Ying Lin, Goichi Miyoshi, Yasuyuki Shima, Gord Fishell, Sacha B. Nelson, and Z. Josh Huang, "A resource of Cre driver lines for genetic targeting of GABAergic neurons in cerebral cortex," *Neuron*, vol. 71, no. 6, pp. 995 1013, 2011.
- [12] Linda Madisen, Theresa A. Zwingman, Susan M. Sunkin, Seung Wook Oh, Hatim A. Zariwala, Hong Gu, Lydia L. Ng, Richard D. Palmiter, Michael J. Hawrylycz, Allan R. Jones, Ed S. Lein, and Hongkui Zeng, "A robust and high-throughput cre reporting and characterization system for the whole mouse brain," *Nature Neuroscience*, vol. 13, no. 1, pp. 133–140, Jan 2010.
- [13] Arthur E. Hoerl and Robert W. Kennard, "Ridge regression: Biased estimation for nonorthogonal problems," *Technometrics*, vol. 42, no. 1, pp. 80–86, 2000.

- [14] Arthur E. Hoerl and Robert W. Kennard, "Ridge regression: Applications to nonorthogonal problems," *Technometrics*, vol. 12, no. 1, pp. 69–82, 1970.
- [15] D. A. Elston and M. F. Proe, "Smoothing regression coefficients in an overspecified regression model with interrelated explanatory variables," *Journal of the Royal Statistical Society, Series C (Applied Statistics)*, vol. 44, no. 3, pp. 395–406, 1995.
- [16] Gene H. Golub, Michael Heath, and Grace Wahba, "Generalized cross-validation as a method for choosing a good ridge parameter," *Technometrics*, vol. 21, no. 2, pp. 215–223, 1979, Publisher: Taylor & Francis https://www.tandfonline.com/doi/pdf/10.1080/00401706.1979. 10489751.
- [17] Janine Bijsterbosch, Stephen M Smith, and Christian Beckmann, An introduction to resting state fMRI functional connectivity, Oxford University Press, 2017.
- [18] Ionas Erb, "Partial correlations in compositional data analysis," Applied Computing and Geosciences, vol. 6, pp. 100026, 2020.
- [19] Jennifer D. Whitesell, Kyle A. Sorensen, Brooke C. Jarvie, Shane T. Hentges, and Nathan E. Schoppa, "Interglomerular lateral inhibition targeted on external tufted cells in the olfactory bulb," *Journal of Neuroscience*, vol. 33, no. 4, pp. 1552– 1563, 2013.
- [20] Matthew A Smith and Marc A Sommer, "Spatial and temporal scales of neuronal correlation in visual area V4," *Journal of Neuroscience*, vol. 33, no. 12, pp. 5422–5432, 2013.
- [21] Cynthia Brewer, Mark Harrower, and The Pennsylvania State University, "Colorbrewer," Accessed: 2020.